

# Zhiqiao Gancao Decoction Ameliorates Hyperalgesia in Lumbar Disc Herniation via the CCL2/CCR2 Signaling Pathway

Zeling Huang\*, Binjie Lu\*, Xianda Zhang\*, Jiangping Wang, Xuefeng Cai, Yujiang Liu, Jianxiong Mo, Yuwei Li, Bo Xu, Xiaofeng Shen

Suzhou TCM Hospital Affiliated to Nanjing University of Chinese Medicine, Suzhou, Jiangsu, 215008, People's Republic of China

\*These authors contributed equally to this work

Correspondence: Bo Xu; Xiaofeng Shen, Suzhou TCM Hospital Affiliated to Nanjing University of Chinese Medicine, Suzhou, Jiangsu, 215008, People's Republic of China, Tel +86 18359146790, Email xubo12080@163.com; 29240818@qq.com

**Purpose:** The aim of this study was to investigate the effect of Zhiqiao Gancao decoction (ZQGCD) on hyperalgesia in lumbar disc herniation (LDH) and its mechanism.

**Methods:** The potential mechanism of ZQGCD's therapeutic effect on LDH was investigated through network pharmacology, which involved screening the targets of eight components that were absorbed into the bloodstream. The effects of CCR2 inhibitors and ZQGCD-containing serum on the excitability of the CCL2/CCR2 signaling pathway and dorsal root ganglion neurons (DRGn) were investigated in vitro. The effects of CCR2 inhibitors and ZQGCD on the expression of the CCL2/CCR2 signaling pathway and ASIC3 in the rat intervertebral disc and dorsal root ganglion (DRG), the degree of disc degeneration, the threshold of foot retreat, and the latency of foot retreat in LDH rats were examined in vivo. The binding affinities and interaction modes between CCR2 and the components absorbed into the blood were analyzed using the AutodockVina 1.2.2 software.

**Results:** Network pharmacology revealed that ZQGCD could treat LDH through a mechanism involving the chemokine signaling pathway. It was observed that the CCR2 inhibitor and ZQGCD-containing serum downregulated CCR2 and ASIC3 expression and decreased cell excitability in DRGn. The CCL2/CCR2 signaling pathway was activated in the degenerated intervertebral disc and DRG of LDH rats, increased the expression of ASIC3, and decreased the mechanical allodynia domain and thermal hyperalgesia domain. However, a CCR2 inhibitor or ZQGCD could ameliorate the above changes in LDH rats. The target proteins, CCL2 and CCR2, exhibited a robust affinity for the eight components that were absorbed into the bloodstream.

**Conclusion:** The CCL2/CCR2 pathway was activated in the intervertebral disc and DRG of LDH rats. This was accompanied by upregulation of ASIC3 expression, increased excitability of DRGn, and the occurrence of hyperalgesia. ZQGCD improves hyperalgesia in LDH rats by inhibiting the CCL2/CCR2 pathway and downregulating ASIC3 expression.

**Keywords:** lumbar disc herniation, dorsal root ganglion neurons, hyperalgesia, traditional Chinese medicine, molecular docking

## Introduction

Lumbar disc herniation (LDH) is a common chronic pain condition that affects people of all ages. LDH cause significant suffering to individuals and imposes a great economic burden on society.<sup>1</sup> Currently, the pathogenesis of LDH is unclear, and there is no specific treatment for the condition. Several studies have reported that pain is the most common clinical symptoms for patients with LDH seeking treatment.<sup>2,3</sup>

LDH-induced mechanical compression and inflammatory immune response are the key factors driving the occurrence of pain, which increase dorsal root ganglion neurons (DRGn) excitability.<sup>4</sup> Increased excitability of DRGn enhances the sensitivity of injurious stimuli induced by dorsal root ganglion (DRG). Ultimately, this leads to hyperalgesia, characterized by a lowered pain threshold, resulting in an elevated increased pain perception when subjected to the same intensity

of stimulation and the induction of pain even under non-painful stimuli.<sup>5</sup> Acid-sensing ion channels (ASICs) are a class of proton-gated cationic channels found primarily in the nervous system. They play an important role in adjusting the pH of body fluids and regulating pain, sour taste, and other physiological functions.<sup>6</sup> ASIC3 on DRG has been linked to pain conduction which is associated with ischemia, inflammation, or tissue acidosis.<sup>7</sup> Chemokines are small molecule secreted proteins with leukocyte chemotactic and cytokine activity. Studies have shown that chemokines and their receptors are involved in various types of chronic pain, such as neuropathic pain, inflammatory pain, cancer pain, among others.<sup>8</sup> The monocyte chemoattractant protein-1 (MCP-1, also known as CCL2) is one of the CC group chemokines that can chemoattract monocytes and stimulate inflammation and immune responses.<sup>9</sup> Previous investigations showed that CCL2 contributes to neuropathic pain at different levels of the peripheral sensory afferent nerve, DRG, spinal cord, and medulla oblongata and facilitates pain conduction.<sup>10</sup> It has also been reported that CCL2 and its receptor type CCR2 (C-C chemokine receptor type 2) participate in the onset and progression of pain.<sup>11</sup>

Traditional Chinese medicine (TCM) has a long history and presents notable benefits, including well-established efficacy, safety, and stability. Extensive research has been conducted to explore the clinical applications of TCM. Zhiqiao Gancao decoction (ZQGCD) is an empirical prescription founded by Professor Gong Zhengfeng, a famous Chinese physician of TCM. Its formula and preparation method are applied under a Chinese national patent (A formula and preparation method of Licorice decoction, patent number: 201910496548.2).<sup>12</sup> In recent years, studies have demonstrated that ZQGCD has remarkable treatment effects on LDH. ZQGCD was found to effectively relieve pain symptoms and improve lumbar function in LDH patients. Animal studies revealed that ZQGCD reduced inflammation levels and inhibited the formation of a local inflammatory microenvironment in LDH rats.<sup>18</sup> It also suppressed the expression of the ASIC3 protein in the spinal cord and DRG and improved hyperalgesia in LDH rats.<sup>12</sup> Analysis of ZQGCD compounds with liquid chromatography-mass spectrometry identified 45 small molecular compounds.<sup>19</sup> In another study, nobiletin, tangeretin, senkyunolide A, glycyrrhetic acid, curcumin, demethoxycurcumin, danshensu, and protocatechuic acid were successfully identified in the blood of LDH rats, indicating that these compounds might be active substances of ZQGCD.<sup>20</sup>

We explored the mechanism of ZQGCD in the treatment of LDH through a combination of network and experimental pharmacology tools. The present study provided compelling evidence that the release of CCL2 was upregulated, leading to the activation of the CCL2/CCR2 signaling system. Subsequently, this activation caused notable modifications in the transcription and functionality of ASIC3, thereby enhancing the excitability of DRGn and establishing the foundation for the initiation and persistence of hyperalgesia in the context of LDH. Furthermore, our investigation demonstrated a clear correlation between the mechanism underlying the therapeutic effect of ZQGCD in alleviating hyperalgesia in LDH rats and the inhibition of CCL2/CCR2 signaling.

## Materials and Methods

### Materials

#### Animals

Sprague-Dawley (SD) rats (male, 160–180 g or 220–250 g) were purchased from Shanghai Slac Laboratory Animal Co., Ltd (Shanghai, China). The rats were housed under controlled conditions (25°C, 50% relative humidity) and allowed free access to food and water. All experimental procedures were performed according to the International Association for the Study of Pain guidelines and were approved by the Medical Ethics Committee of Suzhou TCM Hospital (2020–040).

#### Experimental Drugs

ZQGCD was used and approved by Suzhou TCM Hospital. It was composed of Fructus aurantii (Zhiqiao) 10g (220712010 Tianling Herbal Decoction Piece Co., LTD, Suzhou, China), Angelicae sinensis radix (Danggui) 10g (220623 Chunhui Tang Co., LTD, Suzhou, China), Radix salviae miltiorrhizae (Danshen) 10g (2021100105 Tongde Pharmaceutical Co., LTD, Guizhou, China), Rhizoma sparganii (Sanleng) 10g (220712010 Chunhui Tang Co., LTD, Suzhou, China), Curcumae rhizome (Ezhu) 10g (220712010 Chunhui Tang Co., LTD, Suzhou, China), Pharbitidis (Heichou) 6g (211110006 Tianling Herbal Decoction Piece Co., LTD, Suzhou, China), Pharbitis purpurea (Baichou) 6g (210910006 Tianling Herbal Decoction Piece Co., LTD, Suzhou, China), and Glycyrrhizae (Gancao) 6g (220503

Chunhui Tang Co., LTD, Suzhou, China). To prepare the mixture, 500 mL of cold water was added to the whole recipe and soaked for 30 min. The mixture was then boiled and fried for about 30 min to reached a volume of 200 mL. Subsequently, 300 mL water was added and boiled until it reached a volume of 200 mL (about 30 min). Two batches of filtrates were mixed, and the filtrate was concentrated into 1 g/mL crude drug using a rotary evaporator. A highly selective CCR2 antagonist, RS504393 (Tocris, Bristol, UK), was dissolved in 40% dimethyl sulfoxide before use.

### Experimental Reagents

The reagents used include fetal bovine serum (16000-044, GIBCO, NY, USA), cell counting Kit-8 (CP002, SAB, CA, USA), EDTA (T1300-100, Solarbio, Beijing, China), hematoxylin-eosin dye solution kit, Immunohistochemical pen, and sodium citrate buffer (KGA224, KGSP10, KGB5001 Jiangsu KGI Biotechnology Co., LTD., Nanjing, China). Neutral resin, xylene, methanol, and ethanol (10004160, 1330-20-7, 67-56-1, 64-17-5, Sinopharmacy Chemical Reagent Co., LTD., Beijing, China), high-temperature resistant plastic dyeing stand, DAB Kit (RAK-2001, DAB-1031, Fuzhou Maixin Biotechnology Development Co., LTD., Fuzhou, China), CCL2, IL-6, TNF-, IL-1 ELISA kit (JEB-13579, LA160102H, LA166601H, LA167616H, Nanjing Lapda Biotechnology Co., LTD., Nanjing, China), SYBR Green I fluorescent dye, AceQ Universal SYBR qPCR Master Mix (Nanjing Nuoweizan Biotechnology Co., LTD., Nanjing, China), RIPA Lysate (P0013C, Shanghai Biyuntian Biotechnology Co., LTD., Shanghai, Shanghai Biyuntian Biotechnology Co., Shanghai Biyuntian Biotechnology Co., Shanghai Biyuntian Biotechnology Co., Shanghai, Shanghai, Shanghai, Shanghai, China), HRP-conjugated Affinipure Goat Anti-Mouse IgG (H+L), -actin Antibody, ASIC3 Antibody (SA00001-2, SA00001-1, 20536-1-AP, A10268 Proteintech Group, Inc., IL, USA). CCL2 Antibody, CCR2 Antibody (DF7577, DF2711 Affinity Biosciences, Inc., OH, USA), ECL Luminescent Liquid, Protein Marker (180-5001, 180-6003 Shanghai Tieneng Technology Co., LTD., Shanghai, China), and BCA Protein Assay Kit (23227 Thermo Fisher Scientific, MA, USA).

### Experimental Instruments

The following instruments were used a CO<sub>2</sub> constant temperature incubator (3111, Thermo Fisher Scientific, MA, USA), biosafety cabinet (BHC-1300IIB2, Suzhou Jinjing Purifying Equipment Co., LTD, Suzhou, China), flow cytometer (Accuri C6, BD, CA, USA), fluorescence microscope (DM6000B, Leica, Wetzlar, Germany), and mechanical pain sensitivity measuring instrument (BME-404, Chinese Academy of Medical Sciences, Beijing, China). Thermal pain sensing instrument (35150-001, Ugo Basil SLR, Italy), electric heating oven (101AS-3, Shanghai Shengxin Scientific Instrument Co., LTD. Shanghai, China), digital Pathology biopsy Scanner (VS200, Olympus, Tokyo, Japan); Tianping (E200 Sartorius Gottingen Germany); Table thermostatic oscillator (THZ-312, Shanghai Jinghong Experimental Equipment Co., LTD., Shanghai, China); ELx800 light absorption enzyme label instrument, ELx50 microporous plate automatic washing machine (BIOTEK, VT, USA), frozen centrifuge (5424R, Eppendorf Hamburg, Germany), thermostatic incubator (GHP-9050N, Shanghai Yiheng Scientific Instrument Co., LTD., Shanghai, China), light cycle 96, enzyme label instrument, Mini-PROTEAN Tetra, PowerPac Power supply (biorad, CA, USA), and chemiluminescence imaging system (Tanon 5200, Shanghai Tieneng Technology Co., LTD., Shanghai, China) were also used in this experiment.

### Network Pharmacology Analysis

Targets of the eight components absorbed into the blood were obtained from the TCM Systems Pharmacology Database and Analysis Platform (TCMSP) and the Bioinformatics Analysis Tool for Molecular mechanism of TCM (BATMAN-TCM) database and related literature. The LDH disease targets were retrieved from the GeneCard, DisGeNET, and MalaCards databases. The intersecting targets, identified as common between the absorbed components and the associated disease, were carefully selected as potential targets for the treatment of LDH using ZQGD. The protein-protein interaction (PPI) network for the potential targets was established using the String database. Cytoscape 3.7.2 software was employed to construct the visual representation of the PPI network and to identify core targets based on the network's Betweenness Centrality values. The enrichment analysis of Gene Ontology (GO) and Kyoto Encyclopedia of Genes and Genomes (KEGG) was conducted using the R software, P-value < 0.05 and FDR < 0.25.

## Preparation of the ZQGCD-Containing Serum

The SD rats in the ZQGCD-containing serum group were administered with ZQGCD (12 mL/kg/d) via gavage, whereas those in the blank serum group were gavaged with the same amount of normal saline for seven days. One hour after the last gavage, 3% of pentobarbital was administered as abdominal anesthesia, and blood was drawn from the abdominal aorta. The blood samples were allowed to stand at room temperature for a duration of 2–4 hours and then centrifuged at 3000 r/min for 15 min. Subsequently, the upper serum was collected and subjected to inactivation in a constant temperature water bath set at 56 °C for a period of 30 min. The resulting serum was then filtered using a 0.22 µm microporous filter membrane, packaged, sealed, and stored in a refrigerator at a temperature of –20 °C for future use.

## Extraction, Culture, and Treatment of DRGn

DRGn were collected from SD rats (two months old) which euthanized in a CO<sub>2</sub> chamber. The spinal column of the T7 to L6 segments of the rat was cut and placed in a dissecting dish containing DMEM. Subsequently, DRG tissues were harvested under a dissecting microscope and transferred to a culture dish. Next, the DRG tissues were dissected after removal of the connective tissue. They were the digested with type I collagenase digestion solution (5 mg/mL) for 30 min in an incubator (95% O<sub>2</sub>, 5% CO<sub>2</sub>, 37 °C) to dissociate the cells. The cell precipitates were filtered through a cell sieve, collected by centrifugation, and counted. Subsequently, the cells were seeded on the cell-culture dish and incubated in an incubator (95% O<sub>2</sub>, 5% CO<sub>2</sub>, 37 °C). Upon achieving 90% growth, the cells were randomly allocated into distinct groups, namely the blank group, CCL2 group, CCR2 inhibitor group, and ZQGCD-containing serum group. Subsequently, the cells were subjected to a 12 h pretreatment with either blank serum, blank serum supplemented with RS504393, or ZQGCD-containing serum at concentrations of 5%, 10%, and 15%. Following the pretreatment, the cells were exposed to CCL2 at a concentration of 1 ng/mL, which served to induce the expression of the CCL2/CCR2 signaling pathway. The cells were then cultured for an additional 24 h (Figure 1).

## Cell Counting Kit-8 (CCK-8) Assay

Initially, 5×10<sup>3</sup> cells/well were seeded in 96-well plates. After 24 h of culture, an intervention was performed in groups. Subsequently, three wells were selected from each group, at both 12 hours after pretreatment and 24 hours after the introduction of CCL2. To estimate cell viability, 10 µl of CCK-8 solution was added to each well. The absorbance (optical density, OD) of each well was measured at 450 nm after 30 minutes.

## Intracellular Ca<sup>2+</sup> Content Assay

The cells were enzymatically digested using trypsin, collected, and suspended in phosphate-buffered saline (PBS). Following this, Fluo-3-AM was added to achieve a final concentration of 10 µmol/L, with a negative control being included. The cells were then incubated in a carbon dioxide incubator for 1 h, gently shaken three times during this period. Subsequently, the cells were centrifuged to remove the excess dye, and were subjected to three washes with calcium-free PBS. Finally, the cells were resuspended in calcium-free PBS. Flow cytometry was used to measure the fluorescence intensity of individual cells from each tube sample, and presented as the F value. In addition, 1% Triton X-100 was added for a 30 min incubation at room temperature, and then 1mmol/L calcium chloride was added for a 10

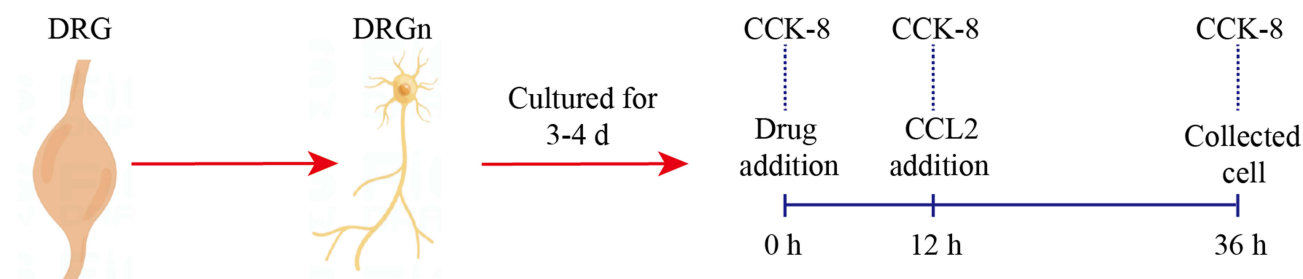


Figure 1 The methodology diagram of cell experimental.

min incubation, and the fluorescence value ( $F_{\max}$ ) was determined. A 10mM EDTA was added and incubated for 10 min, and the fluorescence value ( $F_{\min}$ ) was determined. The  $\text{Ca}^{2+}$  concentration was calculated using the following formula ( $K_d=390\text{nM}$ ).

$$[\text{Ca}^{2+}]_{\text{free}} = K_d \frac{[F - F_{\min}]}{[F_{\max} - F]}$$

## Measurement of the Cell Membrane Potential

Cells were digested using trypsin and collected. The  $10\mu\text{M}$  probe solution was diluted with PBS at 1:100 to obtain a 100 nM staining solution. The cells were suspended in a staining solution, and the concentration was adjusted to  $3 \times 10^5$  cells / mL. Subsequently, the cells were incubated at  $37^\circ\text{C}$  for 15 min in the dark. Finally, the cells were washed once with PBS and analyzed by flow cytometry.

## Immunofluorescence

Cells were fixed with 4% paraformaldehyde, permeabilized with 1% Triton X-100, and blocked with 3% goat serum. The CCR2 antibody (1:500) and ASIC3 antibody (1:100) were added and incubated overnight at  $4^\circ\text{C}$ . This was followed by incubation with the secondary antibody for 30 min. Finally, the cells were counterstained with DAPI and observed under a fluorescent microscope.

## Establishment of a Rat Model of LDH and Treatment

A total of 60 SD rats were randomly divided into the modeling group (50 rats) and sham operation (10 rats). The rats were anesthetized with 1 mL/kg of 3% pentobarbital administered intraperitoneally. The hair on the back of the rats was shaved using a hair shaver, and the coccygeal vertebra was clipped at the tail base about 1 cm from the anus. The nucleus pulposus (NP) and soft tissue around the intervertebral disc of the coccygeal vertebra were removed, and the wound was sutured. A longitudinal incision was made in the middle of the back with the L5 spinous process as the center. The sacrospinous muscles were stripped along both sides of the spinous process and divided on either side to expose the bilateral L4 and L5 lamina (in the sham operation group, the wounds were sutured here). 21G puncture needle was used to puncture the posterior longitudinal ligament and fibrous annulus of L4-L5 and L5-L6 intervertebral discs. The L4 and L5 spinous processes and the right lamina were excised, and the extracted autologous NP was gently placed in the epidural space corresponding to the L4-L5 nerve roots to prevent compression of the spinal cord and nerve roots. Finally, the wound was sutured.<sup>21</sup> The rats were fed in a single cage for three days after the operation, and the tail wound was essentially closed and crusted.

Once the LDH rat model was successfully established, the rats were randomly divided into five groups, with 10 rats in each group. The following treatments were then administered: Sham, no drug intervention; LDH, no drug intervention; LDH+RS504393, the inhibitor RS504393 was injected intraperitoneally at 1 mg/kg, once a day for one week five days after modeling; LDH+ZQGCD, rats were treated for five days after modeling, and the other three groups were gavaged with 3 g/kg, 6 g/kg and 12 g/kg of ZQGCD for three weeks. The recommended daily dosage of ZQGCD for adults is typically 68 g. Considering that the dosage equivalence for rats is approximately 6.3 times that of humans, and accounting for the body weight ratio between humans (70 kg) and animals, the normal daily dosage for rats would be 6 g/kg. In the experimental design, the low-dose group corresponds to half of the normal dosage, while the high-dose group corresponds to twice the normal dosage.<sup>22</sup>

The mechanical allodynia test and thermal hyperalgesia test were conducted at various time points: before modeling, as well as on days 7, 14, 20, and 25 post-modeling. Following the completion of the drug intervention, the rats were anesthetized via intraperitoneal injection of 3% pentobarbital, and blood samples were collected from the abdominal aorta. Subsequently, the dorsal skin and muscle were carefully dissected to expose the lamina. The lamina was exposed using bone masser forceps and the enlarged L4-L6 DRG tissue and intervertebral disc tissue were quickly separated. A portion of the intervertebral disc tissue was fixed in 4% paraformaldehyde for 48 hours to prepare paraffin specimens. The remaining tissue was stored in a refrigerator at low temperature. (Figure 2).

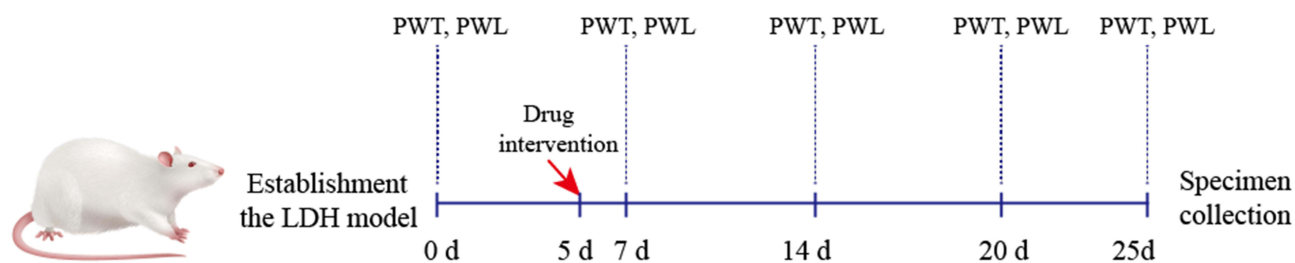


**Figure 2** The methodology diagram of animal experimental.

## Behavioral Testing

### Mechanical Allodynia Test

The Von Frey hair method was used to assess mechanical allodynia, defined as the 50% paw withdrawal threshold (PWT). Von Frey wire was used to test the foot shrinkage threshold daily at 11:00 AM ( $25 \pm 2^\circ\text{C}$  at room temperature, quiet environment). The rats were placed in a  $15 \times 20 \times 15$  cm metal cage. When the rat exploration activities disappeared, 2.00g, 4.00g, 8.00g, 16.00g, 26.00g, 60.00g, and 100 g von Frey were used to stimulate the hind paws so that the pins were S-shaped. Rapid foot retraction for 6–8 s, licking of the affected foot, or neighing were positive reactions, and foot retraction caused by physical activities was not considered positive. The minimum number of grams to achieve at least five positive reactions was used as the threshold for foot contraction. Initially, the stimulation was started using the minimum amount of stimulation and then the intensity of stimulation was increased gradually.

### Thermal Hyperalgesia Test

The thermal sensitivity surface of the hind paw plantar surface was evaluated by measuring the paw retraction latency (PWL). The thermal pain stimulator was placed under the metal grid measuring  $0.5\text{cm} \times 0.5\text{cm}$ , and the rats were placed on the metal grid, with the thermal light source directed at the plantar palm of the hind limb of the rats. An electronic stopwatch was used to record the time from the beginning of thermal radiation irradiation to the retraction of the hind limb. This time was considered the incubation period of thermal stimulation claw retraction response. The maximum duration of the thermal stimulation was set to 20s to prevent substantial damage to the rats from the thermal light source. The light source was automatically turned off if the rats failed to lift their legs 20s after receiving the light source stimulation. Each rat was tested five times, at intervals of 5 min. Results were presented average values.

### Hematoxylin-Eosin (HE) Staining

After routine dewaxing, sections were stained with hematoxylin staining solution for 3 min and washed with water for 1 min. Subsequently, the color separation solution was transferred for about 1 min and washed with water for 1 min. The sections were stained with eosin solution for 2 min and rinsed with running water for 5 min. Finally, the sections were dehydrated, dried, and sealed with neutral glue. The histological structure of each section was observed under a light microscope, and histological grading was performed. The score includes four items: annulus fibrous structure, a boundary line between annulus fibrous and NP, matrix in NP, and cells in NP. Each item is scored from 1 to 3, with a minimum total score of 4 and a maximum total score of 12.<sup>23</sup> Higher scores indicated a greater degree of disc pathology.

### Immunohistochemistry

The expression of CCL2 and CCR2 in the intervertebral disc was demonstrated by immunohistochemical staining. For routine dewaxing and water infiltration of the sections, the slices on a high-temperature resistant plastic staining stand were placed in a staining box containing antigen retrieval buffer. Subsequently, the box was subjected to microwave heating at medium-high intensity for 10 min. After 10 min, the staining box was removed from the microwave and immersed in running water (do not take the slide out of the buffer to cool). Subsequently, the box was soaked in PBS for 3 min, 100ul of 1% BSA was added, and the box was incubated at room temperature for 20 min. After incubation, the sealer was removed but not washed. Next, 100ul of the primary antibody was dropped and incubated overnight at

4°C. Subsequently, the box was immersed in PBS for 3 min × 3 times before adding 50ul of sheep anti-rabbit/rat polymer and incubating in a warm wet box for 20 min. After incubation, the box was again immersed in PBS for 3 min × 3 times, and two drops of freshly prepared DAB solution were added to each sheet. The color depth was observed under the microscope. The color reaction was terminated with distilled water. The sections were put into the hematoxylin dye solution, stained for 2 min, and rinsed with distilled water. Following encapsulation, the protein expression in tissue cells was examined using an optical microscope. Six regions displaying high expression were selected and captured for preservation. To conduct semi-quantitative analysis, Image J software was utilized to measure the average optical density.

## Detection of CCL2, IL-6, TNF- $\alpha$ and IL-1 $\beta$ in Serum by Enzyme Linked Immunosorbent Assay (ELISA)

According to the ELISA kit instructions, the standard substance was diluted by a gradient to draw the standard curve. Set blank holes, standard holes, and sample holes; each hole 3 repeats. After adding samples successively, the film was coated and incubated at 37°C for 90 min. The orifice plate was cleaned, coated with working antibody solution, and incubated for 60 min. The pore plate was cleaned again, coated with enzyme binding solution, and incubated for 30 min. Following plate washing, a color-developing solution was added to the wells. The plate was then incubated in darkness for a period of 15 min, following which a stopping solution was added. The OD 450 value was detected using an enzyme-labeled instrument.

## Measurement of Protein Expression Levels of CCL2, CCR2 and ASIC3 in DRG Were Detected by Western Blot

The samples were weighed, and RIPA lysate was added at 100 mg/200 ul and ground with a ball mill for 15 min. The ground cells were left on ice for 30 min, and the supernatant was obtained through centrifugation at 4°C. The BCA method determined the protein concentration, and the protein denaturation apparatus was boiled and stored at -20°C. According to protein concentration, sample electrophoresis was added, bromophenol blue was finished at the bottom of the glue, and wet transferred to the PVDF membrane. The film was washed with TBST and blocked with 5% skim milk powder at room temperature. The CCL2 antibody (1:1000), CCR2 antibody (1:1200), ASIC3 antibody (1:1500), and  $\beta$ -actin antibody (1:5000) were added and incubated overnight at 4°C. The second antibody was replaced the next day, incubated at room temperature for 2 h, and exposed to the ECL chromogenic solution. Results  $\beta$ -actin was used as an internal mixed quantitative calculation.

## Reverse Transcription-Quantitative Real-Time PCR (RT-qPCR)

Total RNA was extracted with Trizol. The OD value of the RNA was determined with a spectrophotometer, the purity of the RNA was evaluated, and quantitative analysis was performed. Prime Script RT reagent Kit 20ul Reagent Kit reverse-transcribed and stored at -20°C. The corresponding gene sequences in GenBank were retrieved, and the primer was designed using Oligo v6.6 software (Shanghai Bioengineering Technical Service Co., LTD.). The cDNA was amplified with the following primers: CCR2 forward, 5'-TGA ACT TGA ATC GTC TGC A-3'; CCR2 reverse, 5'-CCT TAT TGG GGT CAG CAC AG- 3'; ASIC3 forward, 5'-CTT GAG GAC ATG TTG TTG GA-3'; ASIC3 reverse, 5'-CAT TCG AGT AAA GAT CAC TGT G-3'; glyceraldehyde 3-phosphate dehydrogenase (GAPDH) forward, 5'-GTC GGT GTG AAC GGA TTT G-3'; GAPDH reverse, 5'-TCC CAT TCTC AGC CTT GAC-3'). 5×Prime Script RT Master Mix 20ul system was amplified, and the results were calculated as  $2^{-\Delta\Delta CT}$  semi-quantitative.

## Molecular Docking Analysis

To analyze the binding affinities and modes of interaction between CCR2 and the components absorbed into the blood, the AutodockVina 1.2.2 software (<http://autodock.scripps.edu/>) was utilized.<sup>24</sup> The molecular structure was retrieved from PubChem Compound (<https://pubchem.ncbi.nlm.nih.gov/>). The 3D coordinates of CCL2 and CCR2

were downloaded from the PDB (<http://www.rcsb.org/pdb/home/home.do>). The compound is designated as a ligand and the CCL2 and CCR2 proteins as receptors. PyMOL 4.3.0 software (<https://pymol.org/>) was used for separation of primitive ligand and protein structures, dehydration and removal of organics. AutodockTools software (<http://mgltools.scripps.edu/downloads>) for hydrogenation, inspection charges, atomic type is specified as AD4 type, calculation gasteiger, and construct the protein structure docking box grid. The compound (small molecule ligand) should determine root, and the twisting bond of the ligand should be selected in AutodockTools. Using AutodockTools software, the format of protein structure and small molecule ligand was converted from “.pdb” to “.pdbqt” for further docking experiments. After docking with Vina, the scores of proteins and compounds were calculated, and the force analysis and visualization from three and two dimensions were carried out using Discovery Studio software.

## Statistical Analysis of Data

The statistical software GraphPad Prism 9.0.0 was used to analyze the data. Data were presented as the Mean and standard deviation for three independent experiments. To compare multiple groups, one-way analysis of variance (ANOVA) was used. Pairwise comparisons were made using Tukey's test.  $P < 0.05$  was considered statistically significant.

## Results

### Network Pharmacology Revealed That the Mechanism of ZQGCD Treatment of LDH Was Related to the Chemokine Signaling Pathway

Following the screening criteria, 274 drug targets and 587 LDH disease targets were identified after removing duplicate data. Among these, 46 targets were common to both the drugs and the LDH disease, indicating their significance as potential targets for ZQGCD in the treatment of LDH. The common gene network for drugs and diseases is shown in [Figure 3A](#). The PPI network of potential target was consisted of 46 sites and 1218 edges. The core targets of the network included TNF, IL6, IL1B, MMP9, PTGS2, CXCL8, STAT3, JUN, CTNBN1, CCL2, among others. ([Figure 3B](#)). GO enrichment analysis showed that 3155 biological processes, 328 cell structures, and 213 molecular functions were involved in ZQGCD treatment of LDH ([Figure 3C](#)). A total of 54 pathways are involved in the potential targets for ZQGCD treatment of LDH. [Figure 3D](#) displays the top 20 pathways that exhibit a high correlation, including the chemokine signaling pathway.

### CCL2 Induced CCR2 and ASIC3 Expression in DRGn, Which is Abolished by CCR2 Inhibitor and ZQGCD-Containing Serum

The effects of the CCR2 inhibitor and ZQGCD on the cell viability of DRGn were examined using CCK-8. After 12 hours of pretreatment with RS504393 and ZQGCD containing serum (5%, 10%, and 15%), there was no change in cell viability, indicating that the CCR2 inhibitor and ZQGCD had no cytotoxic effect on DRGn. After adding CCL2 for 24 h, the viability of unpretreated cells decreased significantly, while that of pretreated DRGn did not change compared to the control group. These results indicate that CCR2 inhibitors and ZQGCD have protective effects on DRGn degeneration induced by CCL2 ([Figure 4A](#)). Immunofluorescence and RT-qPCR results showed that adding CCL2 in unpretreated cells and culturing them for 24 h increased the expression of CCR2 and ASIC3. On the other hand, pretreatment with CCR2 inhibitors and ZQGCD-containing serum decreased CCR2 and ASIC3 expression induced by CCL2 ([Figure 4B-D](#)).

### CCR2 Inhibitors and ZQGCD Containing Serum Can Inhibit the Increased Excitability of DRGn Induced by CCL/CCR2 Signaling Pathway

Flow cytometry results showed that the calcium content and cell membrane potential of unpretreated cells increased significantly after adding CCL2 to the culture for 24 h, indicating that the CCL2/CCR2 signaling system can increase the excitability of DRGn. Compared to the CCL2 group, the pretreated DRGn showed a lower calcium content and cell membrane potential, and decreased cell excitability. The results indicated that CCR2 inhibitors and ZQGCD medicated serum could inhibit the increase of excitability of DRGn induced by CCL2/CCR2 signaling system ([Figure 5](#)).



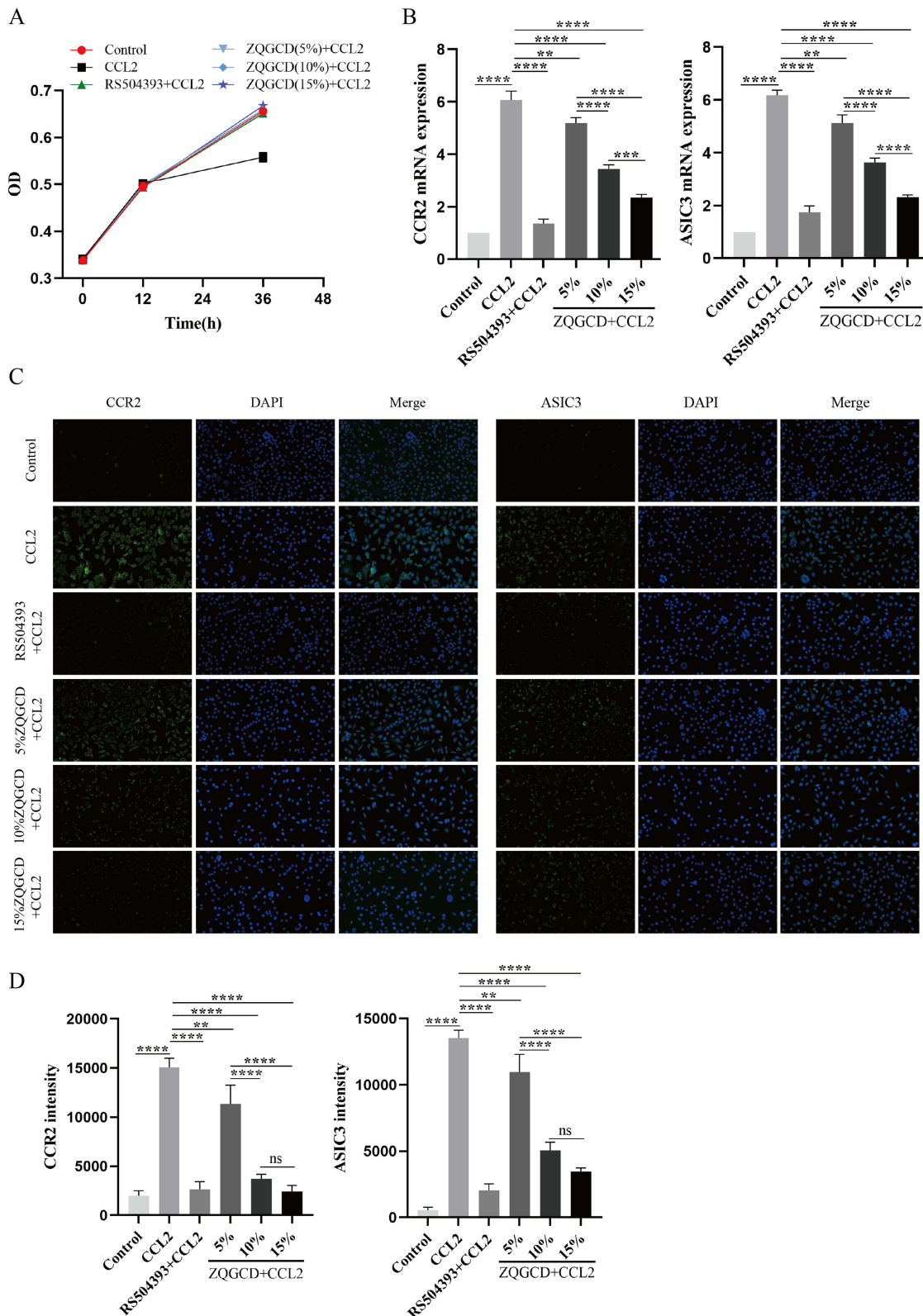


**Figure 4** CCL2 induces the expression of CCR2 and ASIC3 in DRGn, which is inhibited by CCR2 inhibitors and ZQGCD containing serum (A) The cell viability of DRGn. After 12 h pretreatment with RS504393 and ZQGCD containing serum (5%, 10%, and 15%), there was no change in cell viability ( $P>0.05$ ). After adding CCL2 for 24 h, the viability of unpretreated cells decreased significantly ( $P<0.05$ ), while that of pretreated DRGn did not change compared with the control group ( $P>0.05$ ). (B) Expression of CCR2 and ASIC3 mRNA in DRGn. (C and D) Expression of CCR2 and ASIC3 proteins in DRGn.  $**P<0.01$ ,  $***P<0.001$ ,  $****P<0.0001$ , ns:  $P>0.05$ .

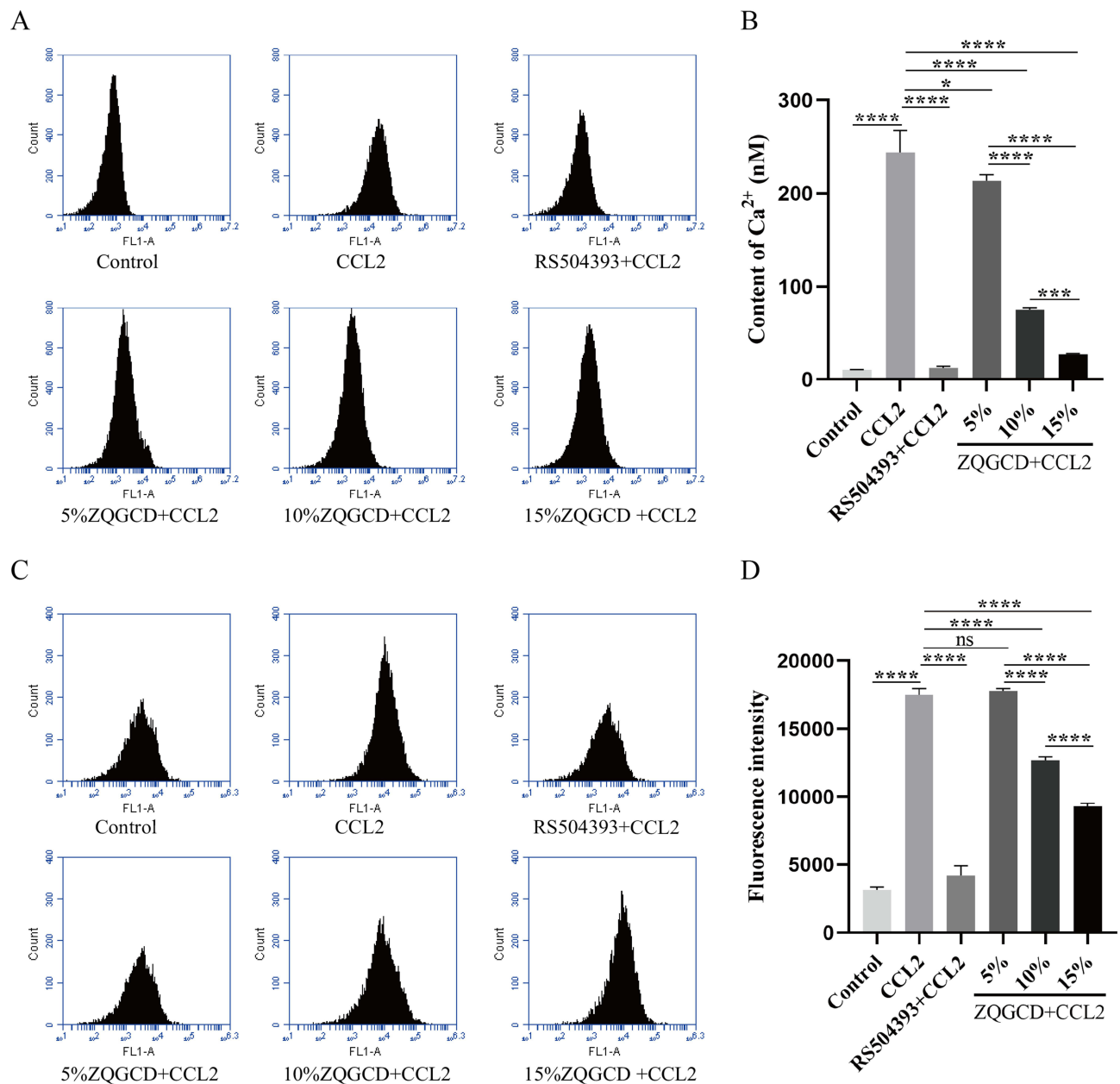


**Figure 5** CCR2 inhibitors and ZQGCD containing serum can inhibit the increased excitability of DRGn induced by CCL/CCR2 signaling pathway. **(A)** Intracellular cationic  $Ca^{2+}$  content. **(B)** DRGn cell membrane potential. \* $P < 0.05$ , \*\*\* $P < 0.001$ , \*\*\*\* $P < 0.0001$ , ns:  $P > 0.05$ .

## CCR2 Inhibitor or ZQGCD Can Improve Hyperalgesia of LDH Rats

On day 7 after NP implantation in LDH rats, the mechanical allodynia and thermal hyperalgesia domains were significantly reduced, lasting until day 25. After RS504393 or ZQGCD treatment, the mechanical allodynia and thermal hyperalgesia domains of LDH rats increased gradually. The results indicated that the CCR2 inhibitor or ZQGCD could improve hyperalgesia in LDH rats (Figure 6).

## CCR2 Inhibitor or ZQGCD Improves Intervertebral Disc Degeneration and Inhibited Serum Inflammatory Cytokines Expression in LDH Rats

HE pathological staining results showed no obvious shrinkage of the NP in the intervertebral disc and complete reticular structure, with a clear boundary with the annulus fibrosus in sham operation rats. In the intervertebral disc of LDH rats,

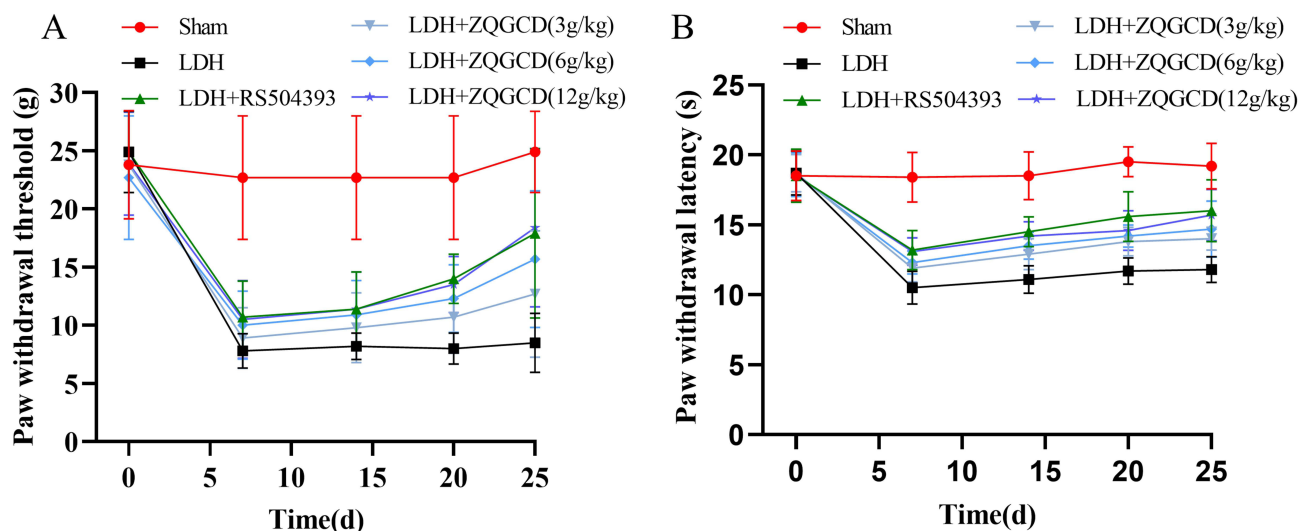


**Figure 6** CCR2 inhibitor or ZQGCD can improve hyperalgesia of LDH rats. **(A)** Paw withdrawal threshold in rats. Compared with sham rats, PWT in LDH rats was significantly lower on day 7 after NP implantation ( $P < 0.0001$ ). After RS504394 and ZQGCD (6 g/kg, 12 g/kg) treatment, the PWT of rats was lower than that of LDH rats at 25 days after NP implantation ( $P < 0.001$ ,  $P < 0.0001$ ). **(B)** Paw withdrawal latency in rats. Compared with sham rats, the PWL in LDH rats was significantly lower on day 7 after NP implantation ( $P < 0.0001$ ). After RS504394 and ZQGCD (3 g/kg, 6 g/kg, 12 g/kg) treatment, the PWL of rats was lower than that of LDH rats at 25 days after NP implantation ( $P < 0.001$ ,  $P < 0.0001$ ,  $P < 0.0001$ ).

the NP was wrinkled and disordered, NP cells were swollen, the boundary between NP was unclear, and the annulus fibrosus was locally torn and disordered. Compared with sham rats, LDH rats showed significantly higher histopathologic scores. Following a three-week treatment with RS504393, significant changes were observed in the intervertebral disc of rats. The NP exhibited signs of shrinkage and disorganization, while NP cells displayed swelling. The boundary between NP and the fibrosus was well-defined, indicating structural integrity of the NP with generally normal fibrosus arrangement. Moreover, the histopathologic scores of the intervertebral disc were significantly lower compared to LDH rats, indicating an improvement in the pathological condition. After 3 weeks of ZQGCD (3 g/kg) treatment, more than half of the NP in the rat intervertebral disc was shrunk, and the structure was disordered. In addition, the boundary between NP and annulus fibrosus was still clear, the annulus fibrosus structure was still complete, and serpentine pattern fibers were present. After three weeks of ZQGCD (6 g/kg, 12 g/kg) treatment, the NP in the rat intervertebral disc was partially shriveled and disorganized and the boundary between NP and annulus fibrosus was clear. The annulus fibrosus structure was complete and arranged normally and serpentine pattern fibers were absent. The histopathologic scores of intervertebral disc were significantly lower than that of LDH rats. These results indicated that CCR2 inhibitors or ZQGCD improved intervertebral disc degeneration in LDH rats (Figure 7A and B).

Analysis of results of serum inflammatory factors showed that CCL2, IL-1 $\beta$ , IL-6 and TNF- $\alpha$  levels in serum from LDH rats were significantly higher after NP implantation but significantly lower after injection of RS504393 or gavage of ZQGCD. These results indicated that CCR2 inhibitors or ZQGCD suppressed inflammation in LDH rats (Figure 7C).

## CCL2/CCR2 Pathway Was Highly Expressed in the Intervertebral Disc of LDH Rats but Inhibited by CCR2 Inhibitor or ZQGCD

The results of immunohistochemical staining of intervertebral disc in rats revealed that compared with Sham rats, the expression of CCL2 and CCR2 in intervertebral disc of LDH rats was significantly higher after NP implantation but significantly lower after injection with RS504393 or gavage with ZQGCD. These results demonstrated that the CCR2 inhibitor or ZQGCD downregulated the expression of proteins associated with the signaling pathway in the intervertebral disc of LDH rats (Figure 8).

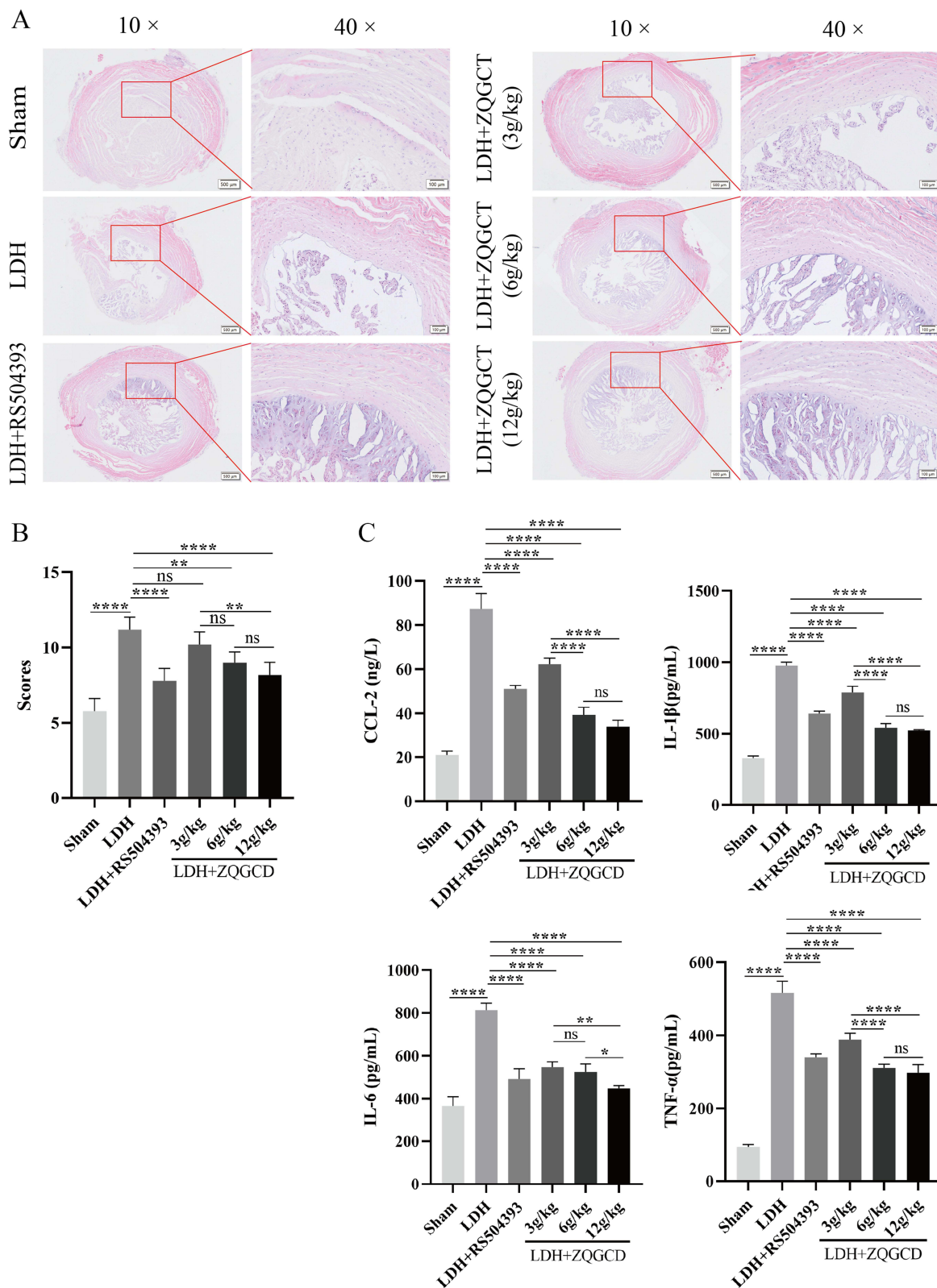


**Figure 7** CCR2 inhibitor or ZQGCD improved intervertebral disc degeneration and inhibited serum inflammatory cytokines expression in LDH rats. **(A)** Representative HE-stained intervertebral disc sections (magnification: 10× or 40×). **(B)** Intervertebral disc histopathologic score. **(C)** Comparison of serum inflammatory cytokines CCL2, IL-1β, IL-6, and TNF-α. \*P<0.05, \*\*P<0.01, \*\*\*P<0.0001, ns: P>0.05.

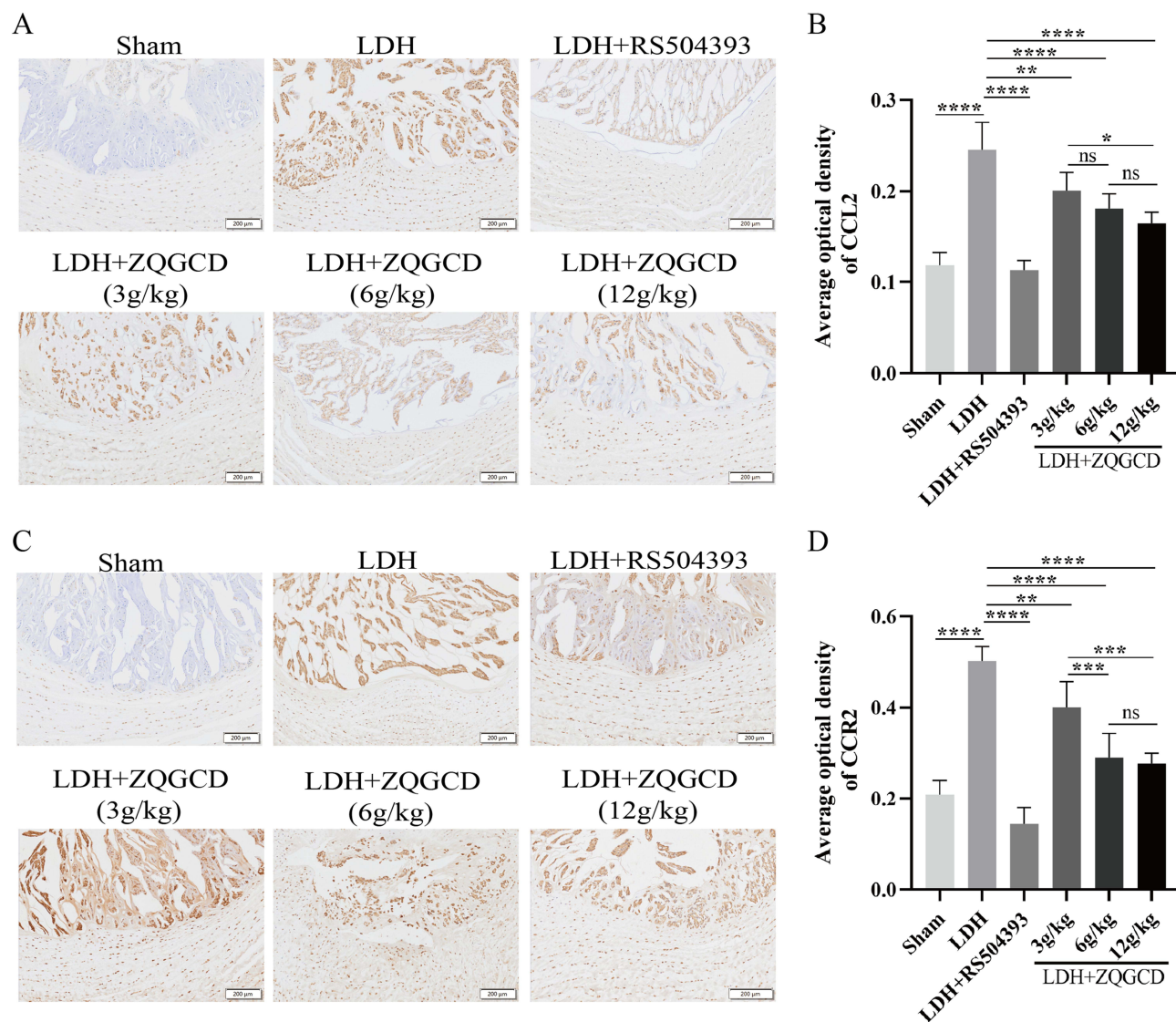


**Figure 8** The expression of CCL2/CCR2 pathway in the intervertebral disc of LDH rats was increased, but CCR2 inhibitors or ZQGCD inhibited this expression. (A and B) Representative images (magnification: 40x) and semi-quantitative histogram of immunohistochemical staining of CCL2 protein of intervertebral disc. (C and D) Representative images (magnification: 40x) and semi-quantitative histogram of immunohistochemical staining of CCR2 protein of intervertebral disc. \* $P < 0.05$ , \*\* $P < 0.01$ , \*\*\* $P < 0.001$ , \*\*\*\* $P < 0.0001$ , ns:  $P > 0.05$ .

## CCL2/CCR2 Pathway and ASIC3 is Highly Expressed in DRG of LDH Rats but Inhibited by CCR2 Inhibitor or ZQGCD

The results of RT-qPCR and Western blot showed that, compared with Sham rats, the expression of CCL2, CCR2 and ASIC3 mRNA and protein in DRG of LDH rats was significantly increased after NP implantation but significantly decreased after injection of RS504393 or gavage with ZQGCD. These results indicated that the CCR2 inhibitor or ZQGCD inhibited the expression of CCL2/CCR2 signaling pathway and ASIC3 in DRG of LDH rats (Figure 9).

## Molecular Docking

Autodock Vina v.1.2.2 was utilized to identify the binding postures and interactions of eight compounds with CCL2 and CCR2 (Figure 10). The binding energies of CCL2 protein with small molecular compounds nobiletin, tangeretin, senkyunolide A, glycyrrhetic acid, curcumin, demethoxycurcumin, danshensu, and protocatechuate were  $-5.5$  kcal/mol,  $-5.5$  kcal/mol,  $-5.5$  kcal/mol,  $-7.3$  kcal/mol,  $-6.0$  kcal/mol,  $-6.2$  kcal/mol,  $-4.9$  kcal/mol, and  $-4.2$  kcal/mol,

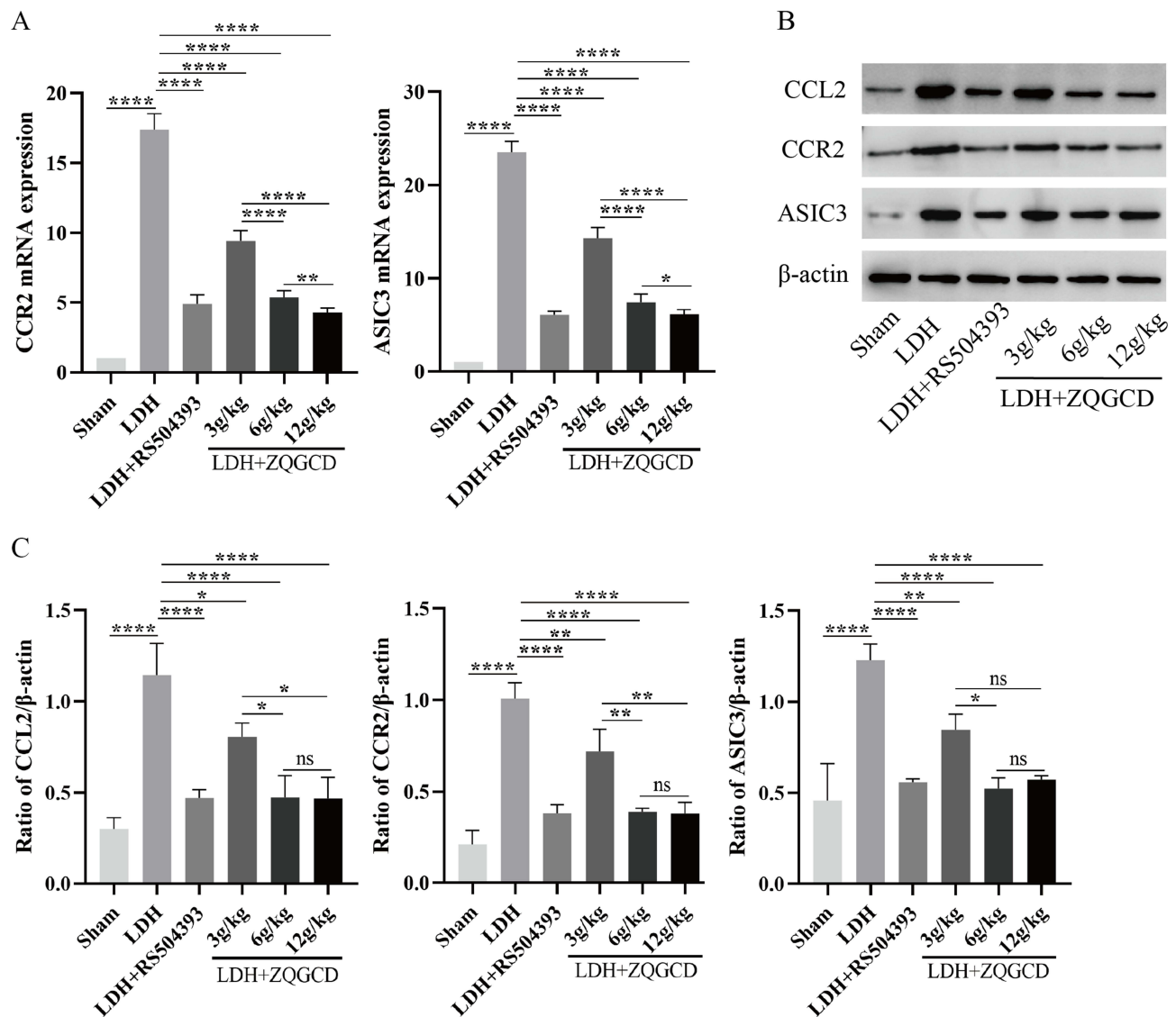


**Figure 9** CCL2/CCR2 pathway and ASIC3 were highly in DRG of LDH rats expressed but inhibited by CCR2 inhibitor or ZQGCD. (A) Bar graphs showing the expression levels of CCL2 and CCR2 mRNA in DRG. (B and C) Immunoblot and bar graphs showing the expression levels of CCL2 and CCR2 in DRG. \* $P < 0.05$ , \*\* $P < 0.01$ , \*\*\* $P < 0.0001$ , ns:  $P > 0.05$ .

respectively. The binding energies of CCR2 protein with small molecular compounds nobiletin, tangeretin, senkyunolide A, glycyrrhetic acid, curcumin, demethoxycurcumin, danshensu, and protocatechuic acid were  $-7.6$  kcal/mol,  $-7.5$  kcal/mol,  $-7.9$  kcal/mol,  $-6.7$  kcal/mol,  $-8.3$  kcal/mol,  $-6.5$  kcal/mol, and  $-6.0$  kcal/mol, respectively. Typically, when the binding energy between a ligand and a target protein is below 0, it indicates a spontaneous binding capability between the ligand and the receptor protein. Moreover, a binding energy value less than  $-5.0$  kcal/mol suggests a strong affinity of the active ingredient with the target protein. Accordingly, the target proteins CCL2 and CCR2 demonstrate a robust affinity with the small molecule compounds.

## Discussion

The CCL2/CCR2 signaling pathway is one of the classical chemokine signaling pathways, which is activated when the nerve is stimulated by inflammation or mechanical injury.<sup>25</sup> When activated, CCL2/CCR2 pathway can directly or indirectly alter the transcription and function of TRPs ion channels,  $K^+$  ion channels, NMDA receptors, and opioid receptor proteins through different intracellular signal transduction pathways, enhance neuronal excitability, increase

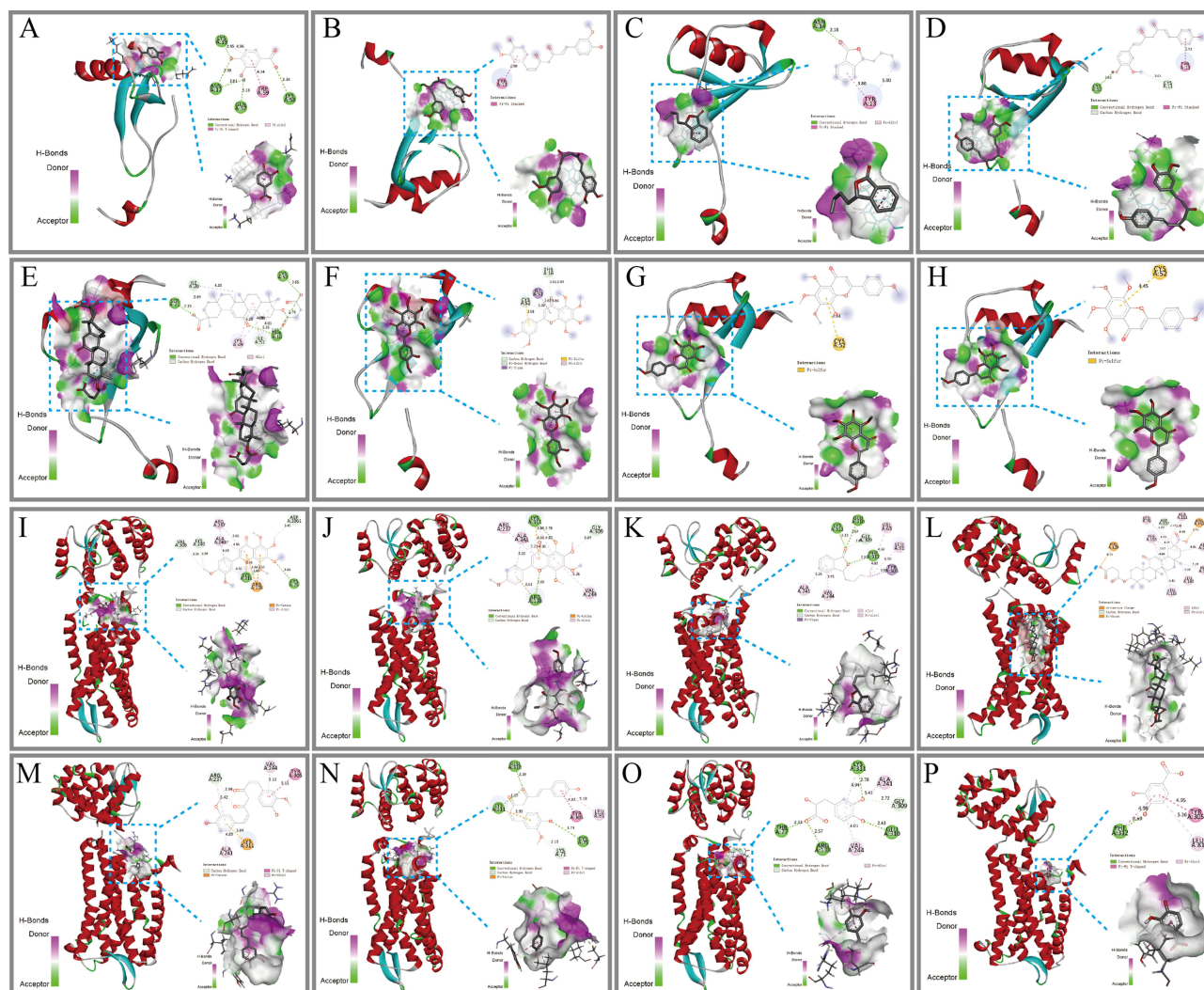


**Figure 10** Molecular docking of CCR2 with compounds in blood. **(A-H)** The binding poses of CCL2 with nobiletin, tangeretin, senkyunolide A, glycyrrhethinic acid, glycyrrhizic acid, curcumin, demethoxycurcumin, danshensu, and protocatechuic acid. **(I-P)** The binding poses of CCR2 with nobiletin, tangeretin, senkyunolide A, glycyrrhethinic acid, glycyrrhizic acid, curcumin, demethoxycurcumin, danshensu, and protocatechuic acid. In the two-dimensional diagram, the green dashed lines represent hydrogen bonds, the light green dashed lines represent carbon-hydrogen bonds, and the pink-brown and purple dashed lines represent hydrophobic forces.

peripheral and central nervous system sensitivity, and generate and maintain pain sensitization.<sup>26</sup> For example, in bone cancer pain rat models, CCL2 was found to activate TRPV1 channels via PI3K/Akt or PLC/PKC signaling pathways, thereby promoting pain transmission via DRG-damaged sensory neurons.<sup>27</sup> In addition, CCL2 also participate in neuropathic pain by selectively upregulating Nav1.8 expression and increasing TTX-R current amplitude.<sup>28</sup> In recent years, there has been increasing research focus on the important role of CCL2 in LDH, which is not only postulated to induce inflammation, but also to directly play a role in establishment of the pain sensitive state of LDH.<sup>29</sup> Intrathecal injection with CCL2 neutralizing antibody or CCR2 antagonist was shown to significantly improve the pain sensitive state of LDH rats.<sup>30</sup> However, no studies have clarified the effect of CCL2 on factors involved in the regulation of hyperalgesia of LDH.

In vitro experiments showed that CCL2 enhanced the excitability of DRGn by inducing the expression of CCR2 and ASIC3. In vivo results using LDH rats showed that inflammation increased the release of CCL2, activated the CCL2/CCR2 pathway in intervertebral disc and DRG, modified the transcription and function of ASIC3, up-regulated ASIC3 in DRG, and activated and maintained hyperalgesia of LDH. Intervertebral disc degeneration and serum inflammatory cytokines were significantly increased in rats but injection with CCR2 inhibitor reversed these changes by inhibiting the

expression of CCL2/CCR2 pathway, further supporting the regulatory role of ASIC3 in the CCL2/CCR2 pathway and the important role of this pathway in the occurrence and development of LDH.

ZQGCD has been included in China's National Famous Medical Secret Prescription for use in then clinical treatment of various lumbar diseases. ZQGCD is composed of Fructus aurantii (Zhiqiao), Angelicae sinensis radix (Danggui), Radix salviae miltiorrhizae (Dansen), Rhizoma sparganii (Sanleng), Curcumae rhizome (Ezhu), Pharbitidis (Heichou), Pharbitis purpurea (Baichou), and Glycyrrhizae (Gancao).<sup>31</sup> We previously found that these eight compounds are released into the blood of LDH rats, which may be responsible for the therapeutic effect of ZQGCD.<sup>20</sup> Nobiletin, tangeretin, senkyunolide A, glycyrrhetic acid, and protocatechuic acid have been shown to have anti-inflammatory and antioxidant effects.<sup>32–35</sup> Curcumin and demethoxycurcumin have been shown to inhibit inflammation and apoptosis of nucleus pulposus cells, and delay intervertebral disc degeneration.<sup>36,37</sup> In various cell lines, curcumin treatment was reported to decrease CCL2 production. In vivo, curcumin reduced CCL2 expression to confer treatment benefits.<sup>38</sup> Our molecular docking results showed that all the aforementioned eight compounds could freely bind to CCR2 protein.

In vitro, ZQGCD-containing serum could inhibit the expression of CCL2/CCR2 pathway and reduce the excitability of DRGn. In vivo experimental results showed that after gavage with ZQGCD, the expression of CCL2/CCR2 pathway in intervertebral disc and DRG of LDH rats was inhibited, the expression of ASIC3 in DRG was decreased, the hyperalgesia and intervertebral disc degeneration of LDH rats were improved, and the expression of serum inflammatory factors was decreased. The effect of ZQGCD was dose-dependent. These results indicate that the mechanism of ZQGCD improves pain sensitivity in LDH rats via the CCL2/CCR2 signaling pathway.

## Conclusion

The activation of the CCL2/CCR2 pathway was observed in the intervertebral disc and DRG of rats with LDH. This activation led to alterations in the transcription and function of ASIC3, resulting in up-regulated expression of ASIC3. Consequently, the excitability of DRG neurons increased, leading to the occurrence of hyperalgesia. Notably, ZQGCD ameliorated hyperalgesia in LDH rats by inhibiting the CCL2/CCR2 pathway and down-regulating ASIC3 expression.

## Data Sharing Statement

The data used to support the findings of this study are included within the article.

## Acknowledgments

We thank Home for Researchers editorial team for language editing service.

## Funding

This work was supported by the National Natural Science Foundation of China (82174399), the Natural Science Foundation of Jiangsu province (BK20211084), Science and technology development plan project of Suzhou (SYS2020183), TCM Science and Technology Development Program of Jiangsu Province (QN202007), and Construction project of Key Laboratory of Bone Injury Science of Traditional Chinese Medicine (JSDW202253, SZS2022019). Jiangsu Province Capability Improvement Project through Science, Technology and Education: Jiangsu Provincial Medical Key Discipline(Laboratory) Cultivation Unit.

## Disclosure

The authors report no conflicts of interest in this work.

## References

1. Benzakour T, Igoumenou V, Mavrogenis AF, Benzakour A. Current concepts for lumbar disc herniation. *Int Orthop*. 2019;43(4):841–851. doi:10.1007/s00264-018-4247-6
2. Samuely-Leichtag G, Eisenberg E, Zohar Y, et al. Mechanism underlying painful radiculopathy in patients with lumbar disc herniation. *Eur J Pain*. 2022;26(6):1269–1281. doi:10.1002/ejp.1947
3. Dower A, Davies MA, Ghahreman A. Pathologic Basis of Lumbar Radicular Pain. *World Neurosurg*. 2019;128:114–121. doi:10.1016/j.wneu.2019.04.147

4. Obata K, Tsujino H, Yamanaka H, et al. Expression of neurotrophic factors in the dorsal root ganglion in a rat model of lumbar disc herniation. *Pain*. 2002;99(1–2):121–132. doi:10.1016/s0304-3959(02)00068-4
5. Lin JH, Chiang YH, Chen CC. Research strategies for pain in lumbar radiculopathy focusing on acid-sensing ion channels and their toxins. *Curr Top Med Chem*. 2015;15(7):617–630. doi:10.2174/1568026615666150217112652
6. Ruan N, Tribble J, Peterson AM, Jiang Q, Wang JQ, Chu XP. Acid-Sensing Ion Channels and Mechanosensation. *Int J Mol Sci*. 2021;22(9):4810. doi:10.3390/ijms22094810
7. Chang CT, Fong SW, Lee CH, Chuang YC, Lin SH, Chen CC. Involvement of Acid-Sensing Ion Channel 1b in the Development of Acid-Induced Chronic Muscle Pain. *Front Neurosci*. 2019;13:1247. doi:10.3389/fnins.2019.01247
8. Jiang BC, Liu T, Gao YJ. Chemokines in chronic pain: cellular and molecular mechanisms and therapeutic potential. *Pharmacol Ther*. 2020;212:107581. doi:10.1016/j.pharmthera.2020.107581
9. Deshmane SL, Kremlev S, Amini S, Sawaya BE. Monocyte chemoattractant protein-1 (MCP-1): an overview. *J Interferon Cytokine Res*. 2009;29(6):313–326. doi:10.1089/jir.2008.0027
10. Singh S, Anshita D, Ravichandiran V. MCP-1: function, regulation, and involvement in disease. *Int Immunopharmacol*. 2021;101(Pt B):107598. doi:10.1016/j.intimp.2021.107598
11. Bianconi V, Sahebkar A, Atkin SL, Pirro M. The regulation and importance of monocyte chemoattractant protein-1. *Curr Opin Hematol*. 2018;25(1):44–51. doi:10.1097/MOH.0000000000000389
12. Shen XF. Inventor; Chongqing Xinlida patent agency, assignee. Zhiqiao Gancao decoction and its preparation method. A kind of formula and preparation method thereof of Fructus Aurantii glycyrrhiza decoction. 2019. China patent CN110101821A.
13. Zhang ZG, Jiang H. Professor Gong Zhengfeng's application of Zhiqiao Gancao decoction in the treatment of lumbar disc herniation. *Chin J Trad Med Traum & Orthop*. 2011;19(12):62.
14. Chen C, Li YW, Chen H. Clinical study on Zhiqiao Gancao decoction for treatment of lumbar disc Herniation. *Acta Chin Med*. 2014;29(05):752–753. doi:10.16368/j.issn.1674-8999.2014.05.052
15. Zhu J, Li YW, Xiang GL, Fang J, Yao Y. Clinical study on Zhiqiao Gancao decoction in patients with lumbar disc herniation after percutaneous intervertebral foraminoscopy. *Hebei J Trad Chin Med*. 2018;40(05):667–672.
16. Cang TS, Chen Y, Li YW. Zhiqiao Gancao decoction combined with lumbar traction for the improvement of lumbar disc herniation. *World Chin Med*. 2020;15(13):1981–1984. doi:10.3969/j.issn.1673-7202.2020.13.025
17. Duan L, Shen XF, Li HW. Clinical effect of traditional Chinese medicine combined with poroscope in treatment of lumbar disc herniation based on MSU classification. *Human J Trad Chin Med*. 2021;37(03):68–71. doi:10.16808/j.cnki.issn1003-7705.2021.03.024
18. Sun JT, Li YW, Shen XF. Effects of Zhiqiao Gancao decoction on inflammation and degeneration of lumbar disc herniation model rats. *J of Emergency in Trad Chin Med*. 2016;25(08):1488–1492. doi:10.3969/j.issn.1004-745X.2016.08.010
19. Shen XF, Li YW, Liang GQ. Anti-inflammatory Effect of Wumen Gancao Decoction on Rats with Lumbar Disc Herniation Associated with Lipid Metabolic Disorder. *Med Plant*. 2019;10(04):24–33. doi:10.19600/j.cnki.issn2152-3924.2019.04.006
20. Shen XF, Li L, Ma QH, et al. Pharmacokinetic study of eight bioactive components following oral administration of Zhiqiao Gancao decoction and observation of its clinical efficacy. *Biomed Chromatogr*. 2020;34(2):e4706. doi:10.1002/bmc.4706
21. Xu W, Ding W, Sheng H, Lu D, Xu X, Xu B. Dexamethasone Suppresses Radicular Pain Through Targeting the L-PGDS/PI3K/Akt Pathway in Rats With Lumbar Disc Herniation. *Pain Pract*. 2021;21(1):64–74. doi:10.1111/papr.12934
22. Chen Q. *Research Methods in Pharmacology of Chinese Materia Medica*. 3rd ed. Beijing: People's Medical Publishing House; 2011:28.
23. Masuda K, Aota Y, Muehleman C, et al. A novel rabbit model of mild, reproducible disc degeneration by an annulus needle puncture: correlation between the degree of disc injury and radiological and histological appearances of disc degeneration. *Spine (Phila Pa 1976)*. 2005;30(1):5–14. doi:10.1097/01.brs.0000148152.04401.20
24. Eberhardt J, Santos-Martins D, Tillack AF, Forli S. AutoDock Vina 1.2.0: new Docking Methods, Expanded Force Field, and Python Bindings. *J Chem Inf Model*. 2021;61(8):3891–3898. doi:10.1021/acs.jcim.1c00203
25. Raghu H, Lepus CM, Wang Q, et al. CCL2/CCR2, but not CCL5/CCR5, mediates monocyte recruitment, inflammation and cartilage destruction in osteoarthritis. *Ann Rheum Dis*. 2017;76(5):914–922. doi:10.1136/annrheumdis-2016-210426
26. Dansereau MA, Midavaine É, Bégin-Lavallée V, et al. Mechanistic insights into the role of the chemokine CCL2/CCR2 axis in dorsal root ganglia to peripheral inflammation and pain hypersensitivity. *J Neuroinflammation*. 2021;18(1):79. doi:10.1186/s12974-021-02125-y
27. Yan Y, Liang Y, Ding T, Chu H. PI3K/Akt signaling pathway may be involved in MCP-1-induced P2X4R expression in cultured microglia and cancer-induced bone pain rats. *Neurosci Lett*. 2019;701:100–105. doi:10.1016/j.neulet.2019.02.024
28. Belkouch M, Dansereau M-A, Réaux-Le Goazigo A, et al. The chemokine CCL2 increases Nav1.8 sodium channel activity in primary sensory neurons through a Gβγ-dependent mechanism. *J Neuroscience*. 2011;31(50):18381–18390. doi:10.1523/JNEUROSCI.3386-11.2011
29. Zhu X, Cao S, Zhu MD, Liu JQ, Chen JJ, Gao YJ. Contribution of chemokine CCL2/CCR2 signaling in the dorsal root ganglion and spinal cord to the maintenance of neuropathic pain in a rat model of lumbar disc herniation. *J Pain*. 2014;15(5):516–26. doi:10.1016/j.jpain.2014.01.492
30. Yu SC, Wu LF, Li XF. Effects of intrathecal injection of CCR2 receptor antagonist on pain and spinal inflammatory factors in rats with lumbar disc herniation. *Jiangsu Pharmaceutical*. 2018;44(05):481–483. doi:10.19460/j.cnki.0253-3685.2018.05.001
31. Gong ZF. Zhiqiao Gancao decoction. *Jiangsu Trad Chin Med*. 2011;43(6):14.
32. Alam F, Mohammadin K, Shafique Z, Amjad ST. Citrus flavonoids as potential therapeutic agents: a review. *Phytother Res*. 2022;36(4):1417–1441. doi:10.1002/ptr.7261
33. Shao M, Lv D, Zhou K, Sun H, Wang Z. Senkyunolide A inhibits the progression of osteoarthritis by inhibiting the NLRP3 signalling pathway. *Pharm Biol*. 2022;60(1):535–542. doi:10.1080/13880209.2022.2042327
34. Richard SA. Exploring the Pivotal Immunomodulatory and Anti-Inflammatory Potentials of Glycyrrhizic and Glycyrrhetic Acids. *Mediators Inflamm*. 2021;2021:6699560. doi:10.1155/2021/6699560
35. Zhang S, Gai Z, Gui T, Chen J, Chen Q, Li Y. Antioxidant Effects of Protocatechuic Acid and Protocatechuic Aldehyde: old Wine in a New Bottle. *Evid Based Complement Alternat Med*. 2021;2021:6139308. doi:10.1155/2021/6139308
36. Cherif H, Bisson DG, Jarzem P, Weber M, Ouellet JA, Haglund L. Curcumin and o-Vanillin Exhibit Evidence of Senolytic Activity in Human IVD Cells In Vitro. *J Clin Med*. 2019;8(4):433. doi:10.3390/jcm8040433.

37. Lu B, Chen X, Chen H, et al. Demethoxycurcumin mitigates inflammatory responses in lumbar disc herniation via MAPK and NF- $\kappa$ B pathways in vivo and in vitro. *Int Immunopharmacol.* 2022;108:108914. doi:10.1016/j.intimp.2022.108914
38. Karimian MS, Pirro M, Majeed M, Sahebkar A. Curcumin as a natural regulator of monocyte chemoattractant protein-1. *Cytokine Growth Factor Rev.* 2017;33:55–63. doi:10.1016/j.cytogfr.2016.10.001

Drug Design, Development and Therapy

Dovepress

### Publish your work in this journal

Drug Design, Development and Therapy is an international, peer-reviewed open-access journal that spans the spectrum of drug design and development through to clinical applications. Clinical outcomes, patient safety, and programs for the development and effective, safe, and sustained use of medicines are a feature of the journal, which has also been accepted for indexing on PubMed Central. The manuscript management system is completely online and includes a very quick and fair peer-review system, which is all easy to use. Visit <http://www.dovepress.com/testimonials.php> to read real quotes from published authors.

Submit your manuscript here: <https://www.dovepress.com/drug-design-development-and-therapy-journal>